

Preparation of NZP-Type $\text{Ca}_{0.75+0.5x}\text{Zr}_{1.5}\text{Fe}_{0.5}(\text{PO}_4)_{3-x}(\text{SiO}_4)_x$ Powders and Ceramic, Thermal Expansion Behavior

D. O. Savinykh^{a,*}, S. A. Khainakov^b, M. S. Boldin^a, A. I. Orlova^a, A. A. Aleksandrov^a, E. A. Lantsev^a, N. V. Sakharov^a, A. A. Murashov^a, S. Garcia-Granda^b, A. V. Nokhrin^a, and V. N. Chuvil'deev^a

^aLobachevsky State University, Nizhny Novgorod, 603950 Russia

^bUniversity of Oviedo, Oviedo, 33003 Spain

*e-mail: savinyhdmitry@mail.ru

Abstract

$\text{Ca}_{0.75+0.5x}\text{Zr}_{1.5}\text{Fe}_{0.5}(\text{PO}_4)_{3-x}(\text{SiO}_4)_x$ ($x = 0-0.5$) solid solutions have been synthesized by a sol-gel process and characterized by X-ray diffraction, IR spectroscopy, and differential scanning calorimetry. As expected, the synthesized phosphatosilicates crystallize in a $\text{NaZr}_2(\text{PO}_4)_3$ -type structure (trigonal symmetry, sp. gr. $R\bar{3}c$). The thermal expansion of the solid solutions has been studied by high-temperature X-ray diffraction in the temperature range from 25 to 800°C. Their thermal expansion parameters have been calculated and analyzed as functions of composition. High-density ceramics based on the $\text{Ca}_{0.875}\text{Zr}_{1.5}\text{Fe}_{0.5}(\text{PO}_4)_{2.75}(\text{SiO}_4)_{0.25}$ phosphatosilicate have been produced by spark plasma sintering and their structure and properties have been studied in detail.

Keywords: NZP, phosphatosilicate, sol-gel process, X-ray diffraction, solid solution, thermal expansion, SPS.

INTRODUCTION

Thermal expansion is an important characteristic of materials for the production of apparatuses, instruments, and mechanisms intended for operation under variable temperature conditions. It is important that materials in contact with each other have similar thermal expansion coefficients, so a search for possibilities of tailoring their thermal expansion is a critical issue.

Compounds that are structural analogs of $\text{NaZr}_2(\text{PO}_4)_3$ (NZP) are promising as key components of materials with tailored physicochemical properties. Well-known members of this family possess high thermal and chemical stability, radiation resistance [1, 2], and ionic conductivity [3–5]; good catalytic [6] and luminescent properties [7, 8]; and low thermal expansion [9–11]. There is ample evidence that they can be used to produce essentially pore-free ceramic materials with good physicochemical properties [2, 12–14].

NZP-type compounds have a framework structure[15]. The key components of the framework are zirconium octahedra (ZrO_6) and phosphate tetrahedral (PO_4), which share oxygens. Groups of two octahedra and three tetrahedra form a three-dimensional framework containing voids, which are predominantly occupied by large, low-charged cations. Compounds with such structure can be described by the general crystal-chemical formula $(\text{M1})^{\text{VI}}(\text{M2})_3^{\text{VIII}}[\text{L}_2(\text{XO}_4)_3]$, where L and M (M1

and M2) represent sites of framework and extraframework atoms, and VI and VIII specify their coordination environment. The M sites can be fully or partially occupied and can remain vacant.

This structure type offers the possibility of varying the composition of compounds over wide ranges without drastic changes in the structural basis of the framework, whereas the properties of the compounds will change significantly [16, 17], which means that their properties can be tailored as required.

The thermal expansion of NZP-type materials has been the subject of extensive studies from the mid-1980s [9, 18, 19] and continues to attract researchers attention [11, 20]. In most cases, heating causes the unit cell of these materials to expand along the crystallographic axis c and contract along the a and b axes (with thermal expansion coefficients $\alpha_c > 0$ and $\alpha_a < 0$). Owing to this feature (thermal expansion anisotropy), many NZP-type materials have small average coefficients of thermal expansion (CTE) [21]. The behavior of NZP materials during heating depends on the nature of the constituent cations (their size, charge, and electronegativity) and is dominated by the contribution of the weakest bonds. Because of this, the cations located on the extraframework site M, as well as the M site occupancy, have a stronger effect [22–24].

The key features of the effect that the composition of the NZP materials has on their thermal expansion are well known. Their coefficient of thermal expansion (CTE) decreases with increasing extraframework cation radius and with decreasing extraframework site occupancy.

In the fabrication of ceramic materials, an important point is the sintering process. Among the known methods for the preparation of ceramic samples, spark plasma sintering (SPS) is of particular interest. The basic principle of this method is rapid heating of powder materials in vacuum or an inert atmosphere by passing high-power dc pulses through equipment and samples, in combination with an applied pressure [25, 26]. Characteristically, ceramic materials produced by SPS have a high relative density and improved physicochemical properties, which opens up new possibilities for the fabrication of ceramic materials for a variety of practical applications [27, 28].

The objectives of this work were to prepare new solid solutions, expected to be isostructural with $\text{NaZr}_2(\text{PO}_4)_3$ and having tailored thermal expansion; measure their thermal expansion as a function of composition; produce ceramics based on the solid solutions; and investigate the mechanical properties of the ceramics.

EXPERIMENTAL

As subjects of investigation, we used $\text{Ca}_{0.75+0.5x}\text{Zr}_{1.5}\text{Fe}_{0.5}(\text{PO}_4)_{3-x}(\text{SiO}_4)_x$ ($x = 0$ – 0.5) solid solutions, in which some of the phosphorus was replaced by silicon to ensure controlled variations in thermal expansion. In addition, we changed the amount of extraframework calcium cations and, accordingly, the M site occupancy.

Powders were synthesized by a sol–gel process, using ethanol as a salting-out agent. Starting chemicals were mixed in stoichiometric ratios. To a 1 M $\text{Ca}(\text{NO}_3)_2$ solution was added a weighed amount of $\text{ZrOCl}_2 \cdot 8\text{H}_2\text{O}$ and a 0.5 M $\text{Fe}(\text{NO}_3)_3$ solution. Next, a 1 M $\text{NH}_4\text{H}_2\text{PO}_4$ solution was added dropwise to the resultant

mixture with constant stirring. This led to the formation of a gel-like precipitate. After that, tetraethyl orthosilicate was added to the system and then ethanol was added to the precipitate. After brief mixing, the gel was dried at 90°C for 24 h. The resultant powder was thermostated at temperatures of 600 and 800°C for 20 h in each step, with intermediate grinding in an agate mortar and X-ray diffraction characterization.

The powders were used to produce ceramics by SPS in a Dr. Sinter Model 625 system (SPS Syntex Inc., Japan). To this end, they were placed in a graphite press die 10.8 mm in inner diameter and heated by high-power millisecond dc pulses (up to 3 kA). The temperature was monitored with a Chino IR-AH pyrometer focused on the surface of the graphite press die. The sintering process was run in vacuum (6 Pa) at an applied uniaxial pressure of 66 MPa.

IR absorption spectra of samples prepared as fineparticle films on KBr substrates were measured in the range 400–1300 cm⁻¹ on a Shimadzu IR Prestige-21 spectrophotometer.

The phase composition of the materials was determined by X-ray diffraction on a Shimadzu LabX XRD6000 X-ray diffractometer in the angular range $2\theta = 10^\circ$ – 50° with CuK α radiation ($\lambda = 1.54056 \text{ \AA}$).

The thermal stability of the structure of the synthesized materials was assessed in the temperature range from 25 to 1000°C at a heating rate of 10°C/min using a SETARAM LABSYS DSC 1600 differential scanning calorimeter.

High-temperature X-ray diffraction data were collected in the temperature range 25–800°C on a PANalytical X'Pert Pro diffractometer equipped with an Anton Paar HTK-1200N high-temperature chamber.

The density of the ceramics was determined by hydrostatic weighing in distilled water on a Sartorius CPA 225D balance. The accuracy in our density measurements was $\pm 0.001 \text{ g/cm}^3$.

The microstructure of the ceramics was examined by scanning electron microscopy (SEM) on a JEOL JSM-6490.

The microhardness (H_V) of the ceramics was measured with a Struers Duramin-5 hardness tester at an indentation load of 2 N. Fracture toughness (K_{Ic}) was calculated by the Palmqvist method from the length of the largest radial crack emanating from an indent made on the ceramics with a Vickers pyramid.

RESULTS AND DISCUSSION

The synthesized samples had the form of brown polycrystalline powders. Figure 1 shows the IR spectra of the samples. The absorption bands in the range 900–1200 cm⁻¹ are attributable to ν_3 asymmetric stretching vibrations of the P–O bonds in the phosphorus tetrahedra. The bands in the range 750–850 cm⁻¹ arise from ν_1 symmetric stretching vibrations, and those in the range 500–700 cm⁻¹ correspond to ν_4 asymmetric bending vibrations.

According to X-ray diffraction data (Fig. 2), the solid solutions under investigation crystallize in a NaZr₂(PO₄)₃-type structure (trigonal symmetry, sp. gr. $R\bar{3}c$ (analog of NaZr₂(PO₄)₃ [15])), as expected.

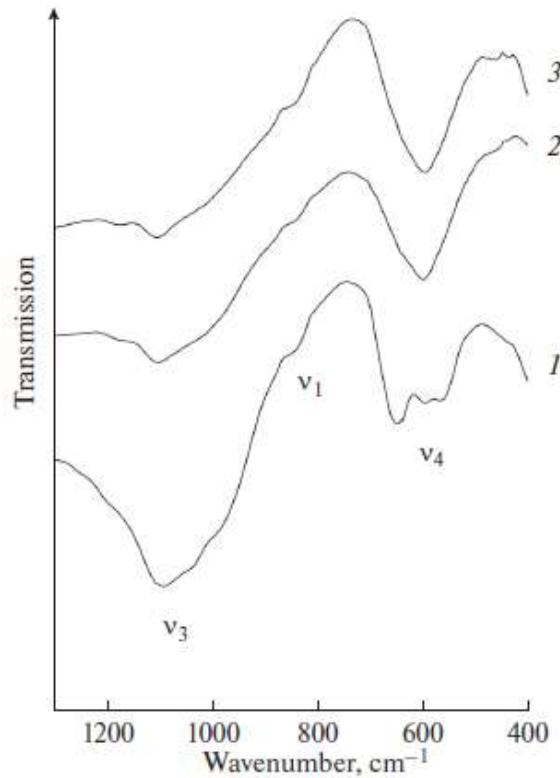


Fig. 1. IR spectra of the $\text{Ca}_{0.75+0.5x}\text{Zr}_{1.5}\text{Fe}_{0.5}(\text{PO}_4)_{3-x}(\text{SiO}_4)_x$ solid solutions with $x =$ (1) 0, (2) 0.25, and (3) 0.5.

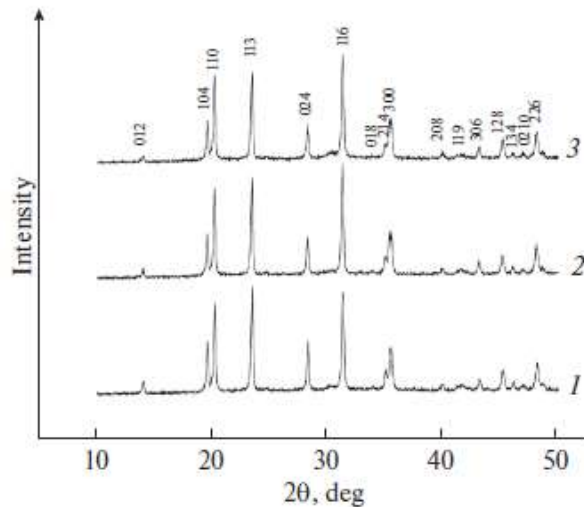


Fig. 2. X-ray diffraction patterns of the $\text{Ca}_{0.75+0.5x}\text{Zr}_{1.5}\text{Fe}_{0.5}(\text{PO}_4)_{3-x}(\text{SiO}_4)_x$ solid solutions with $x =$ (1) 0, (2) 0.25, and (3) 0.5.

The plots in Fig. 3 illustrate the composition dependences of the unit-cell parameters for the solid solutions under consideration. It is seen that there is a tendency for the a cell parameter to increase and the c cell parameter to decrease with increasing silicon content.

The differential scanning calorimetry (DSC) results in Fig. 4 demonstrate that the $\text{Ca}_{0.875}\text{Zr}_{1.5}\text{Fe}_{0.5}(\text{PO}_4)_{2.75}(\text{SiO}_4)_{0.25}$ ($x = 0.25$) and $\text{CaZr}_{1.5}\text{Fe}_{0.5}(\text{PO}_4)_{2.5}(\text{SiO}_4)_{0.5}$ ($x = 0.5$) samples are stable in the temperature range from 25 to 1000°C. Any phase transition similar to that of the $\text{Ca}_{0.75}\text{Zr}_{1.5}\text{Fe}_{0.5}(\text{PO}_4)_3$ ($x = 0$) phosphate [29] was not detected.

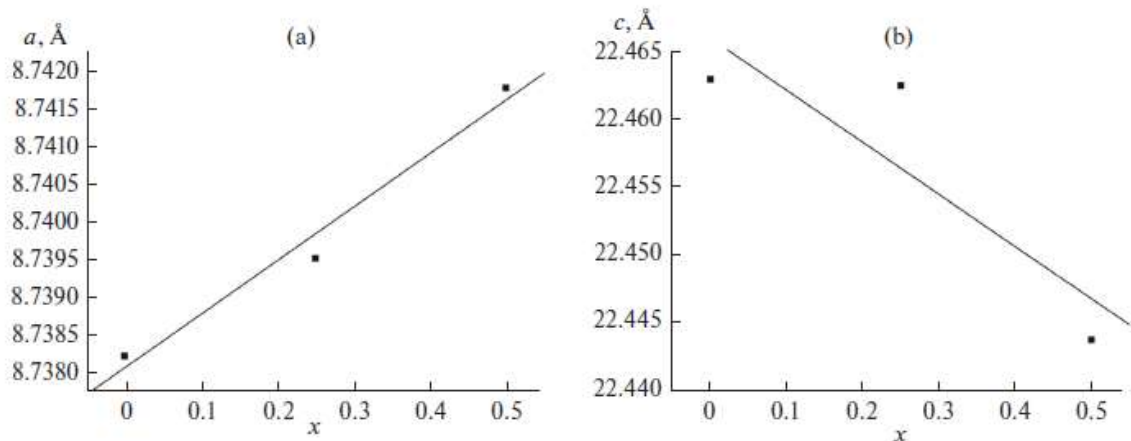


Fig. 3. Composition dependences of the unit-cell parameters (a) a and (b) c for the $\text{Ca}_{0.75+0.5x}\text{Zr}_{1.5}\text{Fe}_{0.5}(\text{PO}_4)_{3-x}(\text{SiO}_4)_x$ solid solutions.

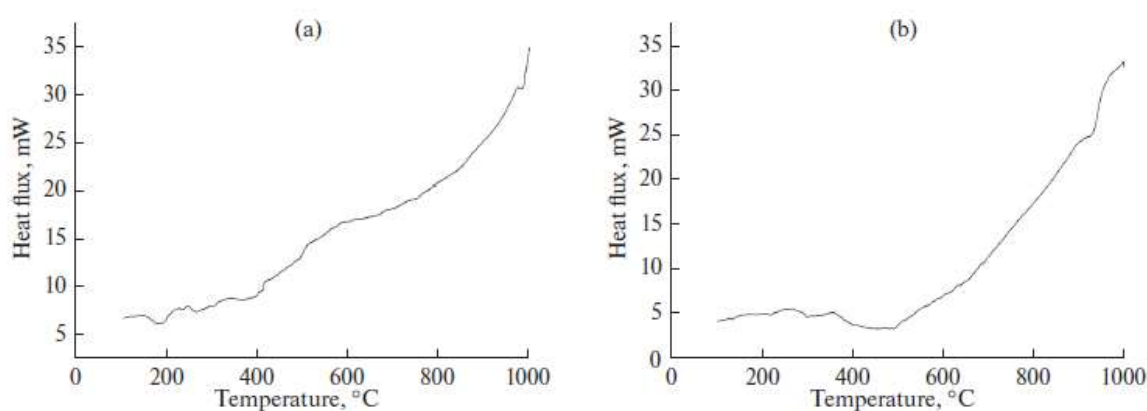


Fig. 4. DSC curves of the $\text{Ca}_{0.75+0.5x}\text{Zr}_{1.5}\text{Fe}_{0.5}(\text{PO}_4)_{3-x}(\text{SiO}_4)_x$ solid solutions with $x =$ (a) 0.25 and (b) 0.5.

Using high-temperature X-ray diffraction, we studied thermal expansion of the synthesized compounds. Figure 5 shows the temperature dependences of their unit-cell parameters. According to the present results, the behavior of the $\text{Ca}_{0.75+0.5x}\text{Zr}_{1.5}\text{Fe}_{0.5}(\text{PO}_4)_{3-x}(\text{SiO}_4)_x$ solid solutions during heating corresponds to that typical of NZP-type compounds: their unit cell contracts in the a and b axis directions and expands along the c axis.

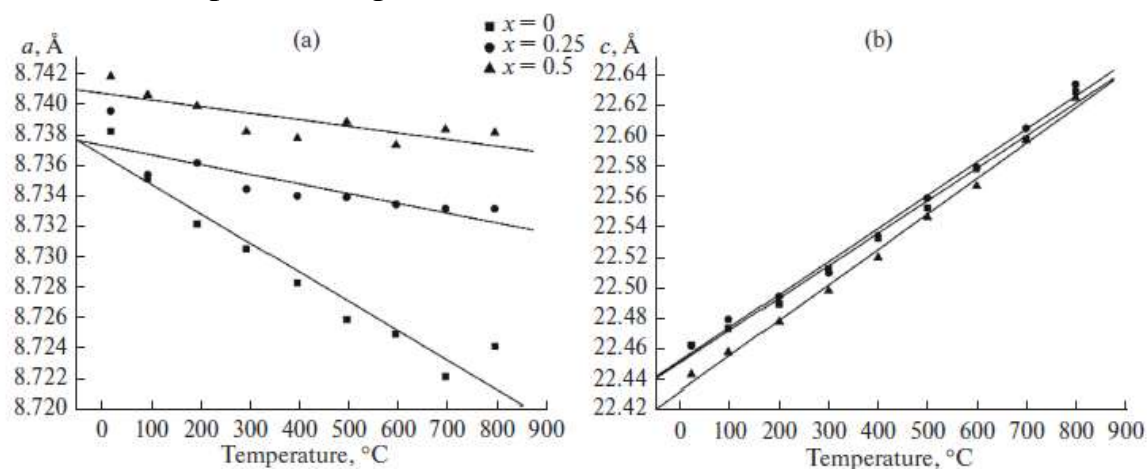


Fig. 5. Temperature dependences of the unit-cell parameters (a) a and (b) c for the $\text{Ca}_{0.75+0.5x}\text{Zr}_{1.5}\text{Fe}_{0.5}(\text{PO}_4)_{3-x}(\text{SiO}_4)_x$ solid solutions with $x = 0, 0.25,$ and 0.5 .

The calculated axial (α_a and α_c), average (α_{av}), and volumetric (β) thermal expansion coefficients and thermal expansion anisotropy ($\Delta\alpha$) of the solid solutions in the temperature range from 25 to 800°C are presented in Table 1 and Fig. 6. Analysis of the present results indicates that the incorporation of silicate groups leads to a sharp decrease in the absolute value of a -axis thermal expansion coefficient and a slight increase in the c -axis coefficient. As a result, thermal expansion anisotropy changes only slightly, whereas the average thermal expansion coefficient increases.

Table 1. Thermal expansion parameters of the $\text{Ca}_{0.75+0.5x}\text{Zr}_{1.5}\text{Fe}_{0.5}(\text{PO}_4)_{3-x}(\text{SiO}_4)_x$ solid solutions.

x	$\alpha_a \cdot 10^6 \text{ }^\circ\text{C}^{-1}$	$\alpha_c \cdot 10^6 \text{ }^\circ\text{C}^{-1}$	$\alpha_{cp} \cdot 10^6 \text{ }^\circ\text{C}^{-1}$	$\beta \cdot 10^6 \text{ }^\circ\text{C}^{-1}$	$\Delta\alpha \cdot 10^6 \text{ }^\circ\text{C}^{-1}$
0	-2.52	9.10	1.35	3.95	11.62
0.25	-0.69	9.67	2.76	8.20	10.36
0.5	-0.46	10.34	3.14	9.36	10.80

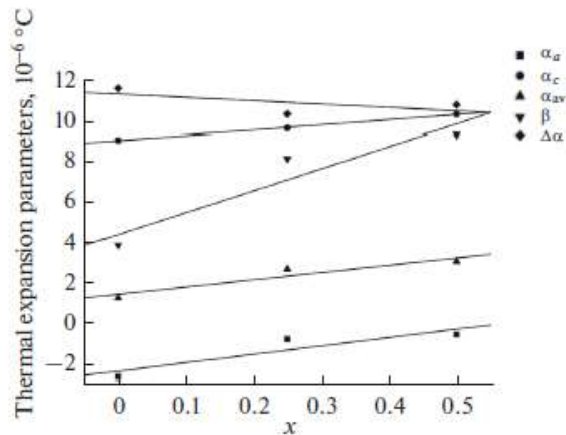


Fig. 6. Composition dependences of the thermal expansion parameters α_a , α_c , α_{av} , β , and $\Delta\alpha$ for the $\text{Ca}_{0.75+0.5x}\text{Zr}_{1.5}\text{Fe}_{0.5}(\text{PO}_4)_{3-x}(\text{SiO}_4)_x$ solid solutions with x from 0 to 0.5.

SPS was used to produce a high-density ceramic from the $\text{Ca}_{0.875}\text{Zr}_{1.5}\text{Fe}_{0.5}(\text{PO}_4)_{2.75}(\text{SiO}_4)_{0.25}$ ($x = 0.25$) powder. Figure 7 shows shrinkage L and shrinkage rate S as functions of heating temperature. It follows from the present experimental data that the powder was sintered in the temperature range from 850 to 1050°C, with a maximum shrinkage rate at 1000°C. The relative density of the resultant ceramic was ~99.7% (the theoretical density of the ceramic is 3.215 g/cm³, as evaluated from the X-ray diffraction data).

The X-ray diffraction data presented in Fig. 8 demonstrate that sintering had little or no effect on the phase composition of the material.

Analysis of scanning electron microscopy data (Fig. 9) indicates that the ceramic has a fine-grained, high-density structure with a grain size ranging from 1 to 3 μm . There is residual microporosity, with a pore size no greater than 0.5 μm .

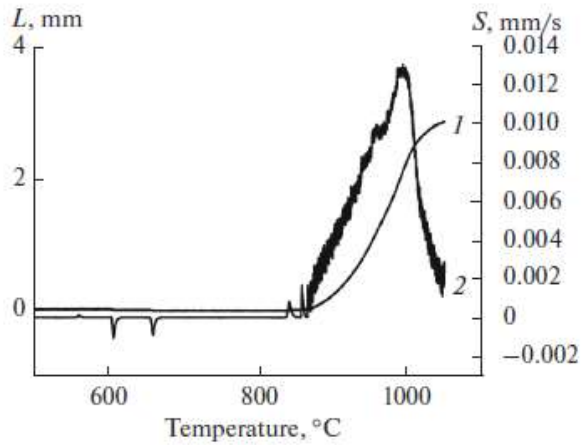


Fig. 7. (1) Shrinkage L and (2) shrinkage rate S as functions of heating temperature for the $\text{Ca}_{0.875}\text{Zr}_{1.5}\text{Fe}_{0.5}(\text{PO}_4)_{2.75}(\text{SiO}_4)_{0.25}$ sample.

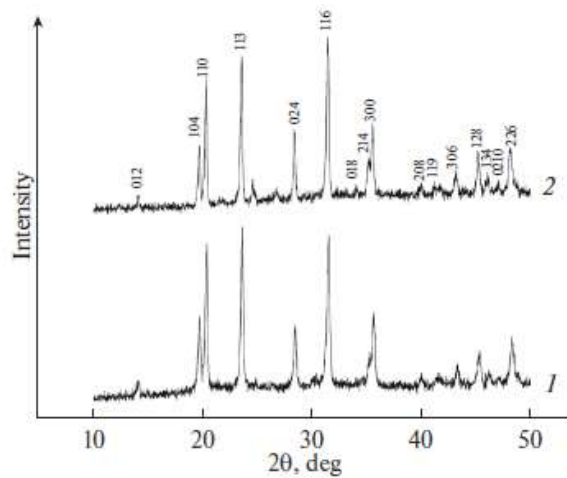


Fig. 8. X-ray diffraction patterns of the $\text{Ca}_{0.875}\text{Zr}_{1.5}\text{Fe}_{0.5}(\text{PO}_4)_{2.75}(\text{SiO}_4)_{0.25}$ sample (1) before and (2) after sintering.

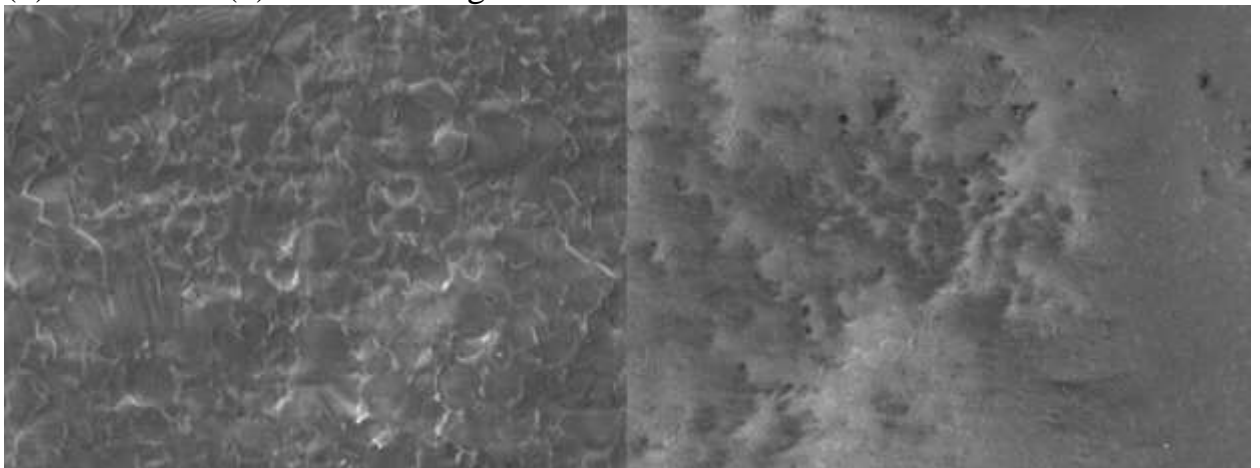


Fig. 9. SEM micrographs of the $\text{Ca}_{0.875}\text{Zr}_{1.5}\text{Fe}_{0.5}(\text{PO}_4)_{2.75}(\text{SiO}_4)_{0.25}$ ceramic sample.

The microhardness (H_V) of the ceramic was determined to be 6.2 GPa, and its fracture toughness (K_{Ic}) was 1.2 $\text{MPa m}^{1/2}$. These microhardness and fracture toughness values are typical of ceramics with the structure type in question [2, 14, 28, 30].

CONCLUSIONS

$\text{Ca}_{0.75+0.5x}\text{Zr}_{1.5}\text{Fe}_{0.5}(\text{PO}_4)_{3-x}(\text{SiO}_4)_x$ ($x = 0-0.5$) solid solutions isostructural with $\text{NaZr}_2(\text{PO}_4)_3$ have been synthesized and characterized. According to the present high-temperature X-ray diffraction data obtained in the range 25–800°C, their lattice parameters a and c are linear functions of temperature: heating reduces the a cell parameter and increases c . The incorporation of silicate groups has been shown to lead to a sharp decrease in the absolute value of a -axis thermal expansion coefficient and a slight increase in the c -axis coefficient. The $\text{Ca}_{0.875}\text{Zr}_{1.5}\text{Fe}_{0.5}(\text{PO}_4)_{2.75}(\text{SiO}_4)_{0.25}$ ($x = 0.25$) and $\text{CaZr}_{1.5}\text{Fe}_{0.5}(\text{PO}_4)_{2.5}(\text{SiO}_4)_{0.5}$ ($x = 0.5$) phosphosilicates have intermediate thermal expansion coefficients: $2 \times 10^{-6} \leq \alpha_{\text{av}} \leq 8 \times 10^{-6} \text{C}^{-1}$.

The observed general trends in the effect of anion substitutions in the framework on the thermal expansion of $\text{NaZr}_2(\text{PO}_4)_3$ -type compounds can be helpful in engineering materials with tailored thermal expansion parameters.

Using one composition as an example, we have demonstrated the possibility of producing ceramic samples with high relative density (~99.7%) and high mechanical strength by SPS.

ACKNOWLEDGMENTS

This work was supported by the Russian Science Foundation, project no. 16-13-10464: Advanced ceramic like mineral materials with improved and adjustable service characteristics: design, synthesis, study.

REFERENCES

1. Orlova, A.I., Volkov, Yu.F., Melkaya, R.F., et al., Synthesis and radiation resistance of NZP-type phosphates containing f-elements, *Radiokhimiya*, 1994, vol. 36, no. 4, pp. 295–298.
2. Orlova, A.I., Volgutov, V.Yu., Mikhailov, D.A., et al., Phosphate $\text{Ca}_{1/4}\text{Sr}_{1/4}\text{Zr}_2(\text{PO}_4)_3$ of the $\text{NaZr}_2(\text{PO}_4)_3$ structure type: synthesis of a dense ceramic material and its radiation testing, *J. Nucl. Mater.*, 2014, vol. 446, pp. 232–239.
3. Goodenough, J.B., Hong, H.Y.-P., and Kafalas, J.A., Fast Na^+ -ion transport in skeleton structures, *Mater. Res. Bull.*, 1976, vol. 11, pp. 203–220.
4. Bykov, D.M., Shekhtman, G.Sh., Orlova, A.I., et al., Multivalent ionic conductivity in the series of phosphates $\text{La}_x\text{Yb}_{1/3-x}\text{Zr}_2(\text{PO}_4)_3$ with NASICON structure, *Solid State Ionics*, 2011, vol. 182, pp. 47–52.
5. Kumar, S. and Balaya, P., Improved ionic conductivity in NASICON-type Sr^{2+} doped $\text{LiZr}_2(\text{PO}_4)_3$, *Solid State Ionics*, 2016, vol. 296, pp. 1–6.
6. Agaskar, P.A., Grasselli, R.K., Buttrey, D.J., and White, B., Structural and catalytic aspects of some NASICON-based mixed metal phosphates, *Stud. Surf. Sci. Catal.*, 1997, vol. 110, pp. 219–226.
7. Orlova, A.I., Kanunov, A.E., Gorshkova, E.N., et al., Synthesis, luminescence, and biocompatibility of calcium- and lanthanide-containing $\text{NaZr}_2(\text{PO}_4)_3$ -type compounds, *Inorg. Mater.*, 2013, vol. 49, no. 1, pp. 89–94.

8. Kanunov, A.E., Glorieux, B., Orlova, A.I., et al., Synthesis, structure and luminescence properties of phosphates $A_{1-3x}Eu_xZr_2(PO_4)_3$ (A—alkali metal), *Bull. Mater. Sci.*, 2017, vol. 40, pp. 7–16.
9. Lenain, G.E., McKinstry, H.A., Limaye, S.Y., and Woodward, A., Low thermal expansion of alkali–zirconium phosphates, *Mater. Res. Bull.*, 1984, vol. 19, no. 11, pp. 1451–1456.
10. Limaye, S.Y., Agrawal, D.K., and McKinstry, H.A., Synthesis and thermal expansion of $MZr_4P_6O_{24}$ (M = Mg, Ca, Sr, Ba), *J. Am. Ceram. Soc.*, 1987, vol. 70, no. 10, pp. 232–236.
11. Volgutov, V.Yu. and Orlova, A.I., Thermal expansion of phosphates with the $NaZr_2(PO_4)_3$ structure containing lanthanides and zirconium: $R_{0.33}Zr_2(PO_4)_3$ (R = Nd, Eu, Er) and $Er_{0.33(1-x)}Zr_{0.25x}Zr_2(PO_4)_3$, *Crystallogr. Rep.*, 2015, vol. 60, no. 5, pp. 721–728.
12. Oikonomou, P., Dedeloudis, Ch., Stournaras, C.J., and Ftikos, Ch., [NZP]: a new family of ceramics with low thermal expansion and tunable properties, *J. Eur. Ceram. Soc.*, 2007, vol. 27, pp. 1253–1258.
13. Sukhanov, M.V., Pet'kov, V.I., and Firsov, D.V., Sintering mechanism for high-density NZP ceramics, *Inorg. Mater.*, 2011, vol. 47, no. 6, pp. 674–678.
14. Orlova, A.I., Koryttseva, A.K., Kanunov, A.E., et al., Fabrication of NZP-type ceramic materials by spark plasma sintering, *Inorg. Mater.*, 2012, vol. 48, no. 3, pp. 313–317.
15. Hagman, L. and Kierkegaard, P., The crystal structure of $NaM_2^{IV}(PO_4)_3$; $Me^{IV} = Ge, Ti, Zr$, *Acta Chem. Scand.*, 1968, vol. 22, pp. 1822–1832.
16. Orlova, A.I., Isomorphism of crystalline $NaZr_2(PO_4)_3$ - type phosphates and radiochemical problems, *Radiokhimiya*, 2002, vol. 44, no. 5, pp. 385–403.
17. Volkov, Yu.F. and Orlova, A.I., *Sistematika i kristallokhimicheskii aspekt neorganicheskikh soedinenii s odnoyadernymi tetraedricheskimi oksoanionami* (Systematics and Crystal-Chemical Aspect of Inorganic Compounds with Mononuclear Tetrahedral Oxyanions), Dimitrovgrad: FGUP “GNTs RF NIAR”, 2004.
18. Roy, R., Agrawal, D.K., Alamo, J., and Roy, R.A., [CTP]: a new structural family of near-zero expansion ceramics, *Mater. Res. Bull.*, 1984, vol. 19, no. 4, pp. 471–477.
19. Alamo, J. and Roy, R., Ultralow-expansion ceramics in the system $Na_2O-ZrO_2-P_2O_5-SiO_2$, *J. Am. Ceram. Soc.*, 1984, vol. 67, no. 5, pp. 78–80.
20. Ribero, D., Seymour, K.C., Kriven, W.M., and White, M.A., Synthesis of $NaTi_2(PO_4)_3$ by the inorganic–organic steric entrapment method and its thermal expansion behavior, *J. Am. Ceram. Soc.*, 2016, vol. 99, no. 11, pp. 3586–3593.
21. Roy, R., Agrawal, D.K., and McKinstry, H.A., Very low thermal expansion coefficient materials, *Annu. Rev. Mater. Sci.*, 1989, vol. 19, pp. 59–81.
22. Lenain, G.E., McKinstry, H.A., Alamo, J., and Agrawal, D.K., Structural model for thermal expansion in $MZr_2P_3O_{12}$ (M = Li, Na, K, Rb, Cs), *J. Mater. Sci.*, 1987, vol. 22, pp. 17–22.

23. Pet'kov, V.I. and Orlova, A.I., Crystal-chemical approach to predicting the thermal expansion of compounds in the NZP family, *Inorg. Mater.*, 2003, vol. 39, no. 10, pp. 1013–1023.
24. Roy, S. and Padma Kumar, P., Framework flexibility of sodium zirconium phosphate: role of disorder, and polyhedral distortions from Monte Carlo investigation, *J. Mater. Sci.*, 2012, vol. 47, pp. 4949–4954.
25. Tokita, M., Development of advanced spark plasma sintering (SPS) systems and its industrial applications, *Ceram. Trans.*, 2006, vol. 194, pp. 51–59.
26. Chuvil'deev, V.N., Boldin, M.S., Nokhrin, A.V., and Popov, A.A., Advanced materials obtained by spark plasma sintering, *Acta Astr.*, 2017, vol. 135, pp. 192–197.
27. Munir, Z.A., Anselmi-Tamburini, U., and Ohyanagi, M., The effect of electric field and pressure on the synthesis and consolidation materials: a review of the spark plasma sintering method, *J. Mater. Sci.*, 2006, vol. 41, pp. 763–777.
28. Potanina, E.A., Orlova, A.I., Nokhrin, A.V., et al., Characterization of $\text{Na}_x(\text{Ca}/\text{Sr})_{1-2x}\text{Nd}_x\text{WO}_4$ complex tungstates fine-grained ceramics obtained by spark plasma sintering, *Ceram. Int.*, 2018, vol. 44, pp. 4033–4044.
29. Savinykh, D.O., Khainakov, S.A., Orlova, A.I., and Garcia-Granda, S., Preparation and thermal expansion of calcium iron zirconium phosphates with the $\text{NaZr}_2(\text{PO}_4)_3$ structure, *Inorg. Mater.*, 2018, vol. 54, no. 6, pp. 591–595.
30. Orlova, A.I., Troshin, A.N., Mikhailov, D.A., et al., Phosphorus-containing cesium compounds with the pollucite structure: fabrication and radiation testing of high-density ceramics, *Radiokhimiya*, 2014, vol. 56, no. 1, pp. 87–92.